International Scholarly Research Network
ISRN Thermodynamics
Volume 2012, Article ID 108781, 8 pages
doi:10.5402/2012/108781

Research Article

Thermodynamics and Oxidation Behaviour of Crystalline Silicon Carbide (3C) with Atomic Oxygen and Ozone

Chandrika Varadachari, Ritabrata Bhowmick, and Kunal Ghosh

Raman Centre for Applied and Interdisciplinary Sciences, 16A Jheel Road, Calcutta 700 075, India

Correspondence should be addressed to Chandrika Varadachari, cv@rcais.res.in

Received 23 September 2012; Accepted 16 October 2012

Academic Editors: Y. Fang, T. M. Inerbaev, and G. Polidori

Thermodynamics of oxidation of crystalline silicon carbide (cubic form) by atomic oxygen (O) and ozone (O_3) was derived to understand the thermodynamic stability of SiC in the upper atmosphere. Equilibrium constants and equilibrium partial pressures were computed for each of eight possible reactions of SiC with O and O_3. Equilibrium activity diagrams were derived, showing the most stable oxidation products of SiC, represented in temperature-oxygen pressure (T-P_{O/O_3}) 2D diagrams. Programs were developed in *Mathematica*. The diagrams provide an understanding of the oxidation routes of SiC under changing levels of O/O_3 and temperature, as encountered during reentry of space vehicles. At high levels of the volatiles, CO_2, CO, and SiO and temperatures between 1000 and 1500 K, oxidation by atomic oxygen or ozone first produced $SiO_2 + C$ followed by $SiO_2 + CO$ and finally $SiO_2 + CO_2$. When volatiles were at very low pressures, the sequence of oxidation was $SiO + CO$ followed by either $SiO_2 + CO$ or $SiO + CO_2$ and finally $SiO_2 + CO_2$. Stability of SiC in ozone was much lower than in atomic oxygen. With both oxidants, the oxidation of the Si in SiC occurred prior to the oxidation of C. Implications for mechanisms of thermal protection are discussed.

1. Introduction

Silicon carbide is an important material for space applications. It is a particularly useful thermal protection system for very high temperature zones like nose-cones in reentry vehicles. Since temperatures may reach 1700°C or higher, oxidation is a major problem and limits the temperatures to which SiC can be used. Several experimental studies on the oxidation of SiC with O_2 have been reported. It was observed [1] that oxidation of SiC between 900–1600°C resulted in a surface layer of SiO_2 that formed a protective film. The oxidation of C-SiC heat shield materials under reentry conditions (50–3500 Pa and 1300–1700°C) showed that a protective SiO_2 layer was formed [2], and oxidation was insignificant as long as this silica layer was present. Others [3] observed etching of the surface and surface segregation of carbon. From photoemission studies on the SiC surface [4], it was concluded that oxygen is incorporated into the Si surface even at the smallest exposures to O_2, but there was no discernible change on the C-terminated surface. Studies have confirmed that the rate controlling process is the diffusion of O_2 through the solid SiO_2 on the surface [5]. Mogilevsky and Zangvil [6] modelled the oxidation of SiC-reinforced mullite–zirconia matrix composites and evaluated oxygen permeabilities of the matrix as well as the silica layer. Oxidation kinetics in the temperature range of 1200–1350°C showed [7] a parabolic behaviour, which indicated a diffusion-controlled mechanism. In high vacuum, the surface composition of α-SiC $(000\bar{1})$ changed as a function of temperature due to oxide formation, yielding graphitic surface carbon [8]. Thermodynamic modelling of the reactions of oxygen with SiC has also been reported [3, 9]. Phase diagrams of Si-C-O (oxygen) system are available in the literature [10, 11] as either triangular diagrams (Si-C-O) or biaxial diagrams (T-SiC/SiO_2).

Three layers of the atmosphere are involved in the oxidation reactions that occur during re-entry, namely, the

Table 1: Reactions of SiC with O and O_3.

	Reactions with atomic oxygen	Reactions with ozone
1	$SiC + 4O \rightarrow SiO_2 + CO_2$	$SiC + 4/3O_3 \rightarrow SiO_2 + CO_2$
2	$SiC + 2O \rightarrow SiO + CO$	$SiC + 2/3O_3 \rightarrow SiO + CO$
3	$SiC + 3O \rightarrow SiO_2 + CO$	$SiC + O_3 \rightarrow SiO_2 + CO$
4	$SiC + 2O \rightarrow SiO_2 + C$	$SiC + 2/3O_3 \rightarrow SiO_2 + C$
5	$SiC + 3O \rightarrow SiO + CO_2$	$SiC + O_3 \rightarrow SiO + CO_2$
6	$SiC + O \rightarrow SiO + C$	$SiC + 1/3O_3 \rightarrow SiO + C$
7	$SiC + 2O \rightarrow Si + CO_2$	$SiC + 2/3O_3 \rightarrow Si + CO_2$
8	$SiC + O \rightarrow Si + CO$	$SiC + 1/3O_3 \rightarrow Si + CO$

troposphere, stratosphere, and mesosphere-lower thermosphere. The troposphere extends to about 18 km at the equator and 8 km at the poles. Tropospheric chemistry would be dominated by oxidation with molecular oxygen whose partial pressures vary from about 0.2 bar to 10^{-3} bar at the tropopause [12, 13]. The stratosphere extends from 15–50 km above the Earth. Atmospheric chemistry of the stratosphere is dominated by ozone, with highest concentrations at 15–30 kilometres above the Earth's surface. Partial pressures of ozone here vary from about $5–30\times10^{-9}$ bar [13]. The mesosphere is located about 50–85 km above Earth's surface, and the lower thermosphere is located between 80 and 180 km. Within this layer, temperature decreases with increasing altitude. Two strong photodissociation continua, the Schumann-Runge continuum, and the weaker Herzberg continuum produce atomic oxygen (O) by breakdown of O_2 [12].

To obtain an understanding of the chemical behaviour of SiC in the upper atmosphere, knowledge of the nature of reactions with atomic oxygen and ozone is important. The objective here was a theoretical investigation of the thermodynamics of oxidation of SiC by O and O_3. Equilibrium constants were computed for all possible reaction pathways. Equilibrium activity diagrams were derived to show the effects of temperature and pressures of O and O_3 on the oxidation of SiC. The resulting diagrams showed the thermodynamically stable oxidation products under variable temperatures and partial pressures of oxidants. Possible pathways of oxidation were proposed. The studies would be useful for modelling chemical transformations of SiC in the stratosphere and mesosphere-lower thermosphere.

2. Theory and Methods

Oxidation of SiC with O/O_3 can occur in eight different ways. These reactions are stoichiometrically represented in Table 1.

Standard free energy change of these reactions at temperature T, ($\Delta G^0_{r,T}$) was obtained from the standard free energy of formation ($\Delta G^0_{f,T}$) as:

$$\Delta G^0_{r,T} = \sum \Delta G^0_{f,T}\ (\text{products}) - \sum \Delta G^0_{f,T}\ (\text{reactants}), \tag{1}$$

which is related to equilibrium constant K as

$$\Delta G^0_{r,T} = -\ RT \ln k = -RT \ln\left(\frac{\Pi a_p^{\nu}}{\Pi a_r^{\kappa}}\right), \tag{2}$$

where a_p and a_r are activities of products and reactants, respectively, and the power terms refer to the stoichiometric amounts of the compounds participating in the reaction. Total free energy change under nonstandard conditions was obtained from the relation:

$$\Delta G_{r,T} = \Delta G^0_{r,T} + RT \ln\left(\frac{\Pi a_p^{\nu}}{\Pi a_r^{\kappa}}\right). \tag{3}$$

Equilibrium activity diagrams were derived from net Gibbs free energy changes ($\Delta G_{r,T}$). This allows us to include the effect of variables (such as partial pressures of CO, CO_2, and SiO) that have important contributions to oxidation. The dominant reaction will be the one with the most negative total free energy change ($\Delta G_{r,T}$).

The process involved (i) computation of free energy changes for all possible reactions in a system, (ii) comparison to obtain the reaction showing greatest reduction in free energy, and (iii) derivation of the limiting conditions for the reaction to have largest free energy reduction compared to all other reactions. Thus, the values of $\Delta G_{r,T}$ for all equations in Table 1 were derived at small intervals of the variables (T-logP_{O/O_3}). These values were compared at each value of the variables, and subsequently boundary conditions were obtained.

Thermodynamic data for the computations were obtained from the literature [14]. Equilibrium activity diagrams showing partial pressure-temperature relations were then computed. For derivation of equilibrium activity diagrams, a program OXID2D was developed in *Mathematica* (see Supplementary Materials available online at doi:10.542/2012/108781). The main program has 2 subroutines (SubOXID_1 and SubOXID_2), which derive the standard free energy change of the oxidation reaction ($\Delta G^0_{r,T}$) and equilibrium ozone (O_3) pressures at lower and higher temperatures T (flow chart in Figure 1). The first sub-routine (SubOXID_1) is for reactions in the lower temperature range (298.15–1900 K), where SiO_2 is in the solid phase; the other sub-routine (SubOXID_2) is for reactions at temperatures above the melting point of SiO_2 (2000–3200 K). Inputs required are the gas constant R (in kJ/mole) and values of logP_{CO_2}, logP_{CO}, and logP_{SiO} (Figure 1). Other input data are temperatures and the corresponding standard free energy of formation ($\Delta G^0_{f,T}$) of all compounds in the reactants and products. Then, for each temperature T, $\Delta G^0_{r,T}$ is derived by (1). The list of temperature-$\Delta G^0_{r,T}$ is exported for the main program. Additionally, equilibrium ozone (O_3) pressures are computed for constant values of logP_{CO_2}, logP_{CO}, and logP_{SiO} and plotted as T versus logP_{O_3}. The subroutines are available as supplementary information.

The main program OXID2D (supplemental file) then derives the equilibrium boundaries from total free energy change of reaction ($\Delta G_{r,T}$) using (3). To compute the values of $\Delta G_{r,T}$, activities of CO_2, CO, and SiO have to be defined.

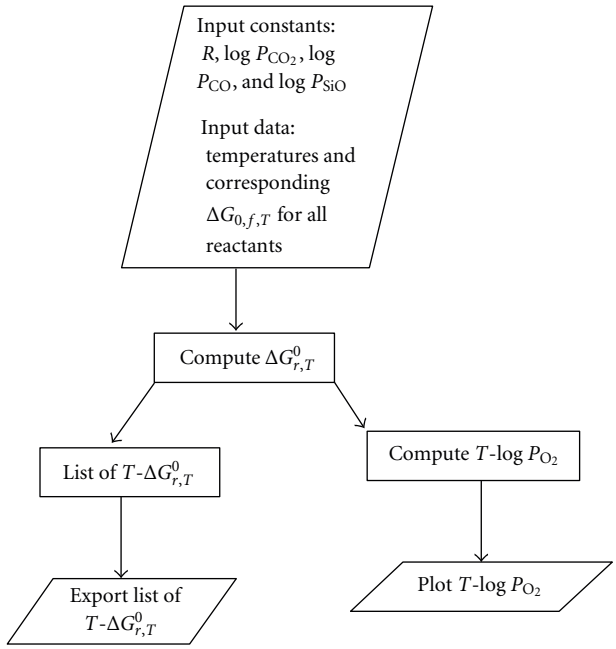

Figure 1: Flowchart for subroutine program SubOXID to compute equilibrium ozone/atomic oxygen activity and standard free energy change of reaction with temperature.

Here, these were assigned constant values representing four different conditions, namely, $P_{CO_2/CO/SiO} = 10^0$, 10^{-3}, 10^{-7}, and 10^{-10}. The next step of the program (flow diagram in Figure 2) defines minimum and maximum temperatures and ozone (O_3) partial pressures ($\log P_{O_3}$) and the respective increment intervals. A list of the variables, T-P_{O_3}, is then generated. The data from SubOXID_1 & 2 are imported, and the relation between T-$\Delta G^0_{r,T}$ is fitted into a linear regression equation. From this equation, $\Delta G^0_{r,T}$ values are derived for every value of temperature increment. Subsequently, using (3), $\Delta G_{r,T}$ values are computed from the values of $\Delta G^0_{r,T}$ using P_{CO_2}, P_{CO}, and P_{SiO} as constants, T and P_{O_3} as variables, temperature range $T =$ 500 to 3200 K, ozone levels $\log P_{O_3} = 1$ to -50, and increment intervals of $T = 5$ K and $\log P_{O_3} = 1$. Only negative values of $\Delta G_{r,T}$ are retained. Derived $\Delta G_{r,T}$ values for all the reactions are combined into separate lists for each T-log P_{O_3}. In each list, the $\Delta G_{r,T}$ values are compared, and the reaction showing the most negative value is assigned to that T-log P_{O3} as the most favourable (stable) reaction. The reaction is identified and represented by a coloured box at that particular value of T-log P_{O_3}. The process is repeated over all values of T-log P_{O_3}, and all points are combined in a single plot. A similar method was earlier used to derive equilibrium diagrams for nonstoichiometric clay minerals in aqueous environments [15] and also to derive fuzzy phase diagrams representing 464 metastable minerals [16].

Equilibrium diagrams in the atomic oxygen system were derived with the same program after substituting the $\Delta G^0_{f,T}$ values for O and changing the reaction stoichiometries according to those shown in Table 1.

Table 2: Equilibrium O, O_3 pressures for oxidation of SiC, Si, and C.

Reaction	1000 K		2000 K		3000 K	
	logP_O	logP_{O_3}	logP_O	logP_{O_3}	logP_O	logP_{O_3}
1	−23.66	−52.61	−9.05	−24.89	−4.20	−15.77
2	−18.22	−36.30	−9.63	−26.64	−6.67	−23.17
3	−24.87	−56.24	−10.04	−27.88	−5.13	−18.54
4	−27.17	−63.15	−9.74	−26.97	−4.01	−15.20
5	−18.82	−38.11	−8.44	−23.07	−4.92	−17.94
6	−16.18	−30.17	−8.61	−23.60	−5.98	−21.11
7	−18.44	−36.95	−7.72	−20.92	−4.29	−16.05
8	−16.85	−32.19	−9.38	−25.89	−7.15	−24.62
9	−19.59	−40.41	−9.88	−27.39	−6.18	−21.72
10	−28.88	−68.27	−10.37	−28.87	−4.11	−15.50
11	−20.26	−42.43	−10.65	−29.69	−7.36	−25.23
12	−20.14	−42.07	−8.35	−22.81	−4.40	−16.35

3. Results and Discussion

3.1. Equilibrium Constants and Equilibrium Gas Pressure. Equilibrium constant (log k)-temperature relationships for 8 types of oxidations of cubic (3C) SiC (Table 1) are presented in Figure 3. log k values were highly positive and suggested that all oxidations were thermodynamically favourable. The oxidation reaction producing $SiO_2 + CO_2$ had highest values of log k for both the oxidants O and O_3. This was followed by SiO_2 + CO and then SiO_2 + C. At higher temperatures, there was a crossover, with SiO + CO_2 having higher log k than SiO_2 + C. In general, reactions producing SiO_2 or CO_2 were energetically more favourable than reactions producing SiO or CO. The value of k reduced sharply with temperature for all reactions except (6) and (8).

Equilibrium constants for reactions with O_3 were generally smaller than with O. Thus, at 1000 K, log k values for the formation of $SiO_2 + CO_2$ from O and O_3 were 94.6 and 70.2, respectively; at 2000 K, these values were 36.2 and 33.2. Oxidation to SiO + CO_2 at 1000 K showed a similar trend with equilibrium constants of 56.3 and 38.0 for reactions with O and O_3, respectively.

Equilibrium partial pressures of O and O_3 for oxidation of SiC (under standard pressures of CO_2, CO and SiO) are presented in Table 2. Oxidation was thermodynamically favourable at 1000 K with log P_O levels as low as -29; reactions forming SiO_2 occurred at lower O pressures than those forming SiO. At 3000 K, equilibrium log P_O levels were about -6 for SiO formation, and unlike trends at 1000 K, SiO_2 was formed at higher O levels compared to SiO. Oxidations with O_3 (Table 2) followed a similar trend. However, equilibrium activities for oxidation with ozone were substantially lower than for atomic oxygen.

Partial pressures of the volatiles, CO_2, CO, and SiO had a significant impact in lowering the pressures of O/O_3 at which oxidation began. Reactions forming SiO (Figure 4) were particularly affected by increasing levels of the volatiles, as observed by the steep slopes. Oxidation to SiO_2 was

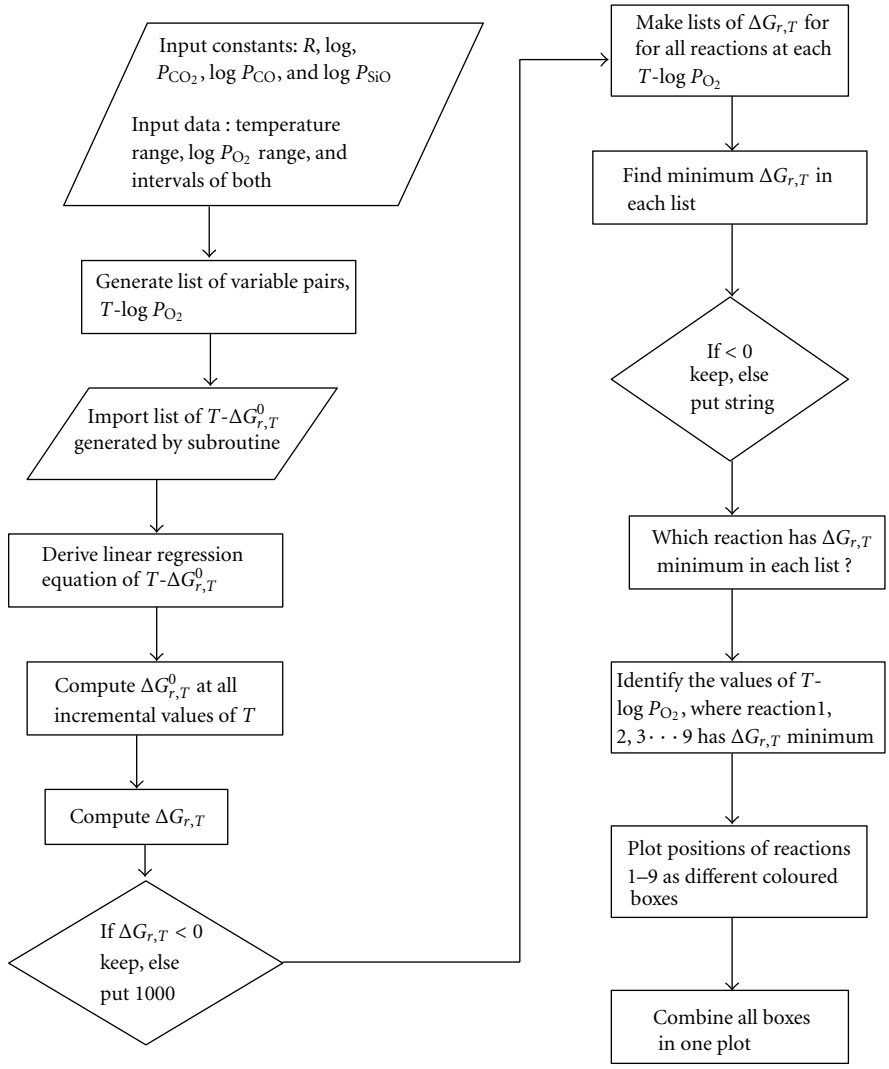

Figure 2: Flowchart for the program OXID2D to derive oxidation phase diagram.

comparatively less affected by the levels of volatile products. This was true for both oxidants, O and O_3. Reactivity of SiC towards ozone was particularly remarkable. Even in the presence of substantial levels of the oxidation inhibitors, oxidation to SiO could occur at O_3 pressures as low as 10^{-30} atm, which is about 10^{17} times lower than the level of atomic oxygen required for the same oxidation.

3.2. Oxidation Equilibrium Diagrams. Reaction equilibrium diagrams of thermodynamically stable products formed, when SiC (cubic) was exposed to various O pressures at different temperatures and different levels of CO_2, CO, and SiO, are presented in Figures 5(a)–5(d). Figure 5(a) shows the nature of products under standard (unit) pressures of gaseous products CO_2, CO, and SiO. At temperatures below 1500 K, as O pressure increased, SiO_2 and C were the first reaction products. On further increase in O pressure, SiO_2 and CO_2 were formed (at $\log P_O \gtrsim -18$). At temperatures above 1500 K, the initial products were SiO_2 + CO followed by SiO_2 + CO_2 at higher O pressures. In the region beyond ~2300 K, oxidation proceeded from SiO + CO to SiO_2 + CO and then to SiO_2 + CO_2. Significantly, the sequence of oxidation also suggested that oxidation of the Si in SiC occurred prior to the oxidation of C.

As levels of CO, CO_2, and SiO were reduced to 10^{-3} atm (Figure 5(b)), the stability zone of SiC was reduced from an upper P_O limit of 10^{-12} to 10^{-18}. Above temperatures of ~1800 K, SiO was the first oxidation product. Further oxidation produced either SiO_2 + CO or SiO + CO_2 depending on whether temperature was above or below 2350 K. Temperature for formation of SiO was greatly lowered as levels of CO, CO_2, and SiO were further reduced (Figures 5(c) and 5(d)). Thus, SiO was formed at ~1100 K when pressures of CO, CO_2, and SiO were at 10^{-10} atm (Figure 5(d)); equilibrium pressure for stability of SiC also dropped sharply to about 10^{-20} atm.

Briefly, at lower temperatures and higher levels of volatiles (Figures 5(a) and 5(b)), oxidation with atomic oxygen first produced SiO_2 + C followed by SiO_2 + CO_2.

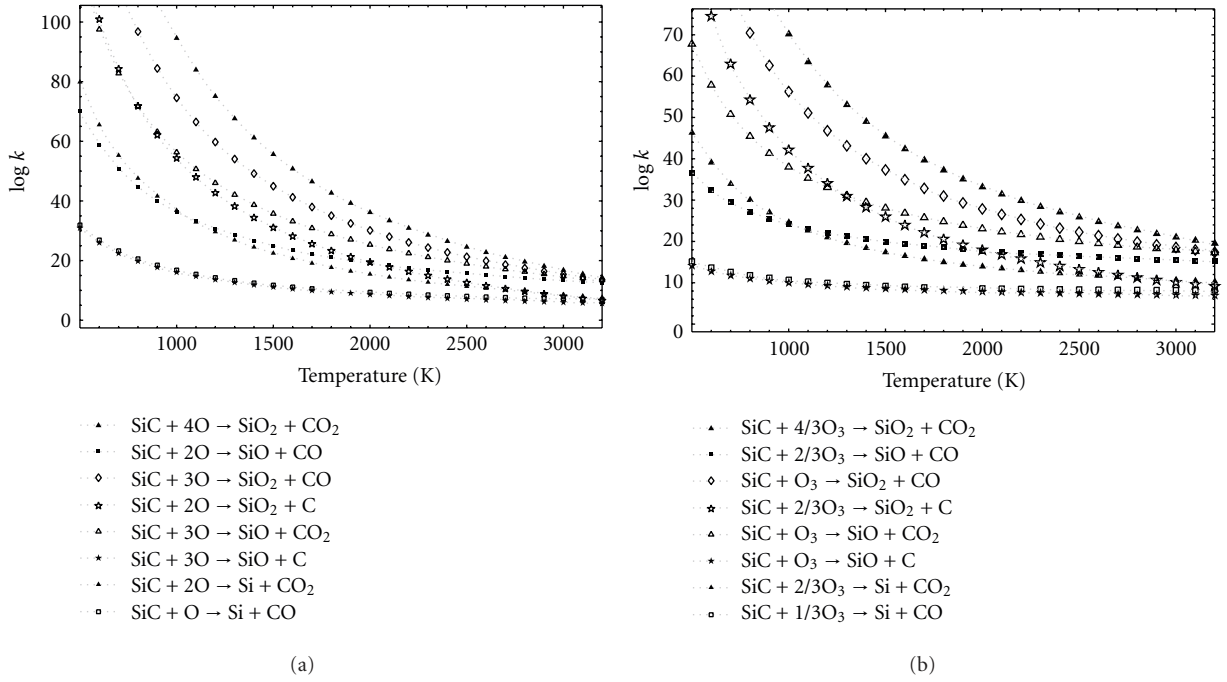

Figure 3: Equilibrium constant (K)-temperature (T) relations for reactions of (a) SiC with O and (b) SiC with O_3.

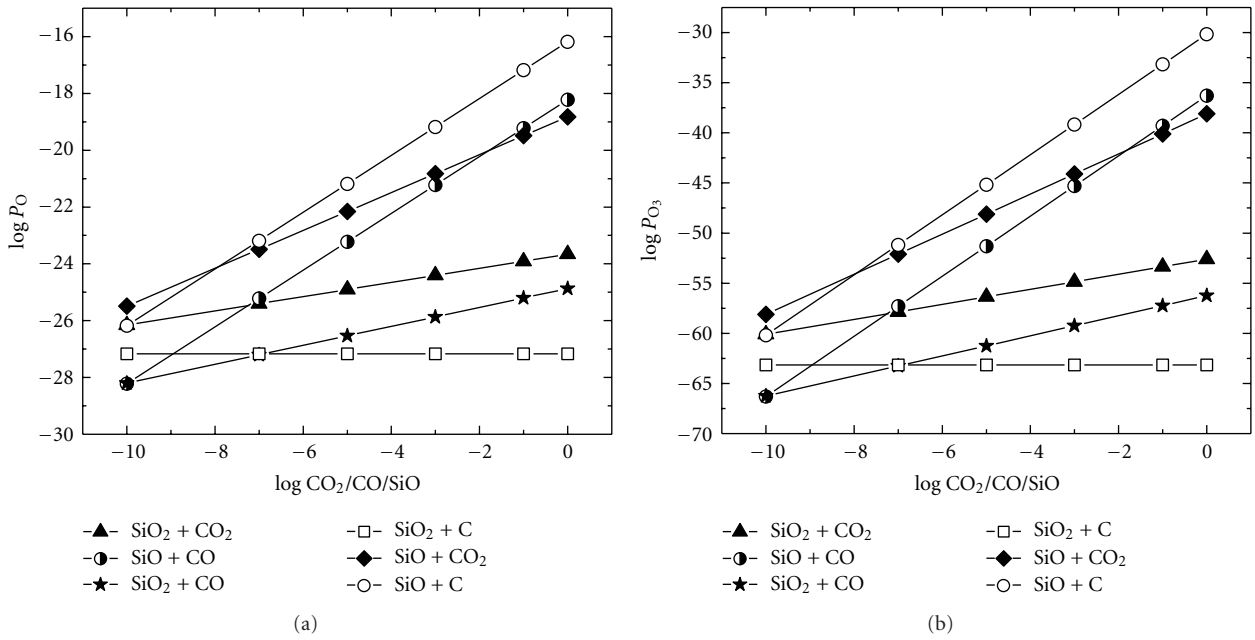

Figure 4: Relationship between equilibrium partial pressures of (a) O and (b) O_3 and partial pressures of CO_2/CO/SiO in oxidation of SiC.

Increasing temperature and reducing pressures of volatiles (Figures 5(c) and 5(d)) resulted in the oxidation sequence SiO + CO then SiO + CO_2 and finally SiO_2 + CO_2. Lower temperatures favoured the formation of SiO_2 (passive oxidation), whereas SiO was formed at higher temperatures (active oxidation).

Stability of SiC in ozone was severely reduced compared to atomic oxygen. Even at $\log P_{CO_2/CO/SiO}$ of −3, SiC oxidised to SiO and CO at 10^{-34} atm O_3 and at 1600 K (Figure 6(b)). There was no observable stability field of SiC (down to $\log P_{O_3} = -50$) when pressures of volatiles were very low (10^{-10} atm, Figure 6(d)). Oxidation products were similar to those observed with molecular and atomic oxygen. However, the stability field of SiO_2 + CO increased significantly. At lower temperatures, oxidation proceeded with the formation of SiO_2 + CO followed by SiO_2 + CO_2. At higher temperatures, SiO + CO formed first; this oxidised to SiO + CO_2 and finally to SiO_2 + CO_2.

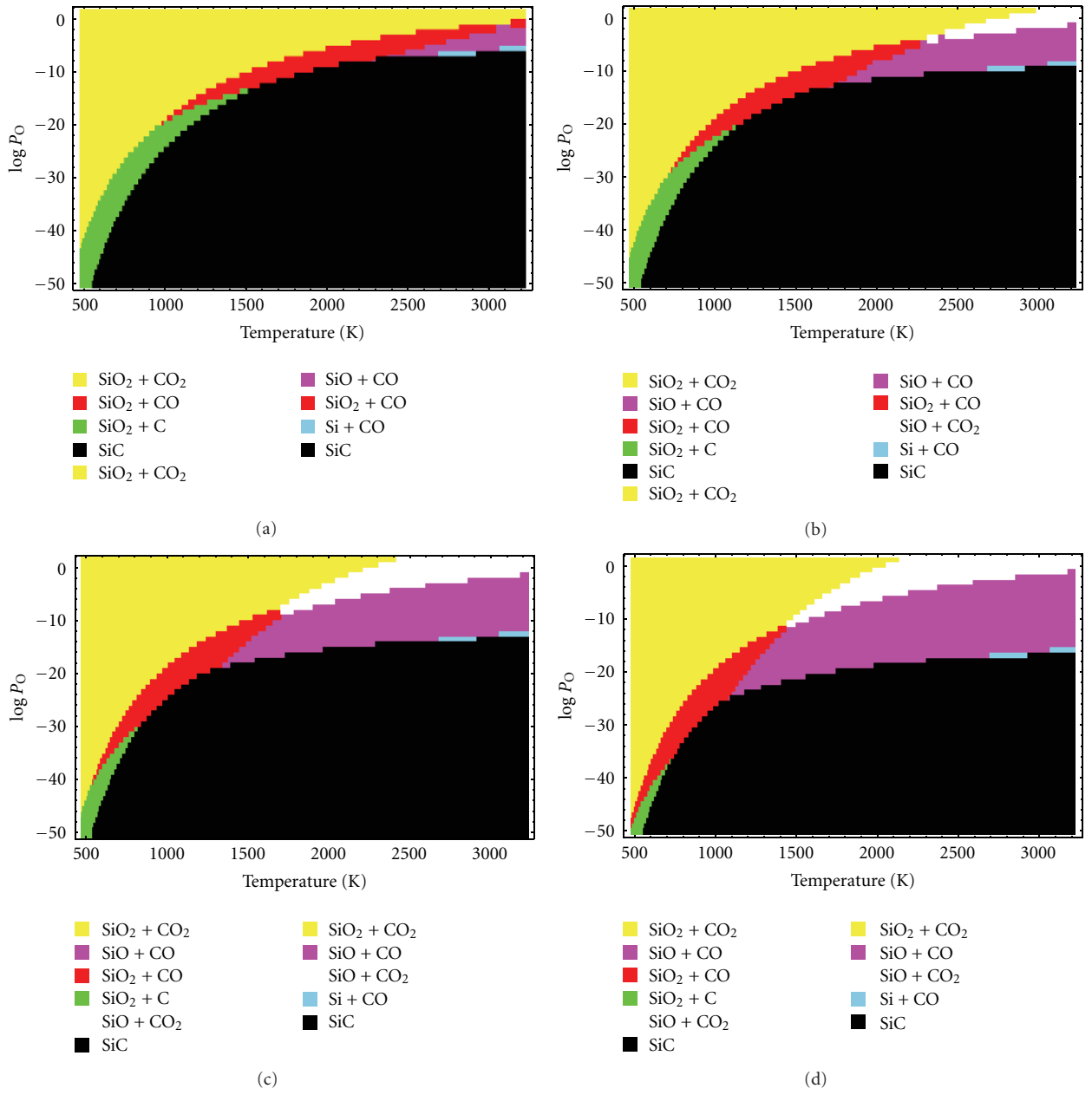

FIGURE 5: Equilibrium diagram of SiC oxidation with atomic oxygen (O) at (a) $\log P_{CO_2} = 0$, $\log P_{CO} = 0$, and $\log P_{SiO} = 0$, (b) $\log P_{CO_2} = -3$, $\log P_{CO} = -3$, and $\log P_{SiO} = -3$, (c) $\log P_{CO_2} = -7$, $\log P_{CO} = -7$, and $\log P_{SiO} = -7$, and (d) $\log P_{CO_2} = -10$, $\log P_{CO} = -10$, and $\log P_{SiO} = -10$.

With regard to reactions at the surface of reentry vehicles, the diagrams suggest that at the initial phase (in the upper mesosphere, where temperatures fall as low as 200 K, and the main oxidant is atomic oxygen) oxidation would mainly produce SiO_2 and CO_2. On entry into the stratosphere, under the conditions of temperature and ozone pressures encountered, SiO_2 and CO_2 would form. Since tropospheric oxygen levels are in the range of 0.2 bar to 10^{-3} bar at the tropopause [4], the implications are that SiO_2 and CO_2 would be the major oxidation products (provided CO/CO_2 levels are high, as in the presence of ablatives). The initial formation of SiO_2 would result in a protective layer that would retard diffusion and further oxidation of SiC. Although in the absence of CO/CO_2 producing ablatives the oxidation product would be SiO, the initial coating of SiO_2 would protect the bulk SiC from complete oxidation. Such a protective mechanism would be effective only below the melting point of SiO_2, that is, 1996 K. Above this temperature, complete oxidation can occur (since wind speeds would be sufficient to blow away the liquid SiO_2 coating).

Experimental data on the oxidation of silicon carbide with ozone showed that oxidation rates in ozone-containing atmosphere were much higher than those in a pure oxygen

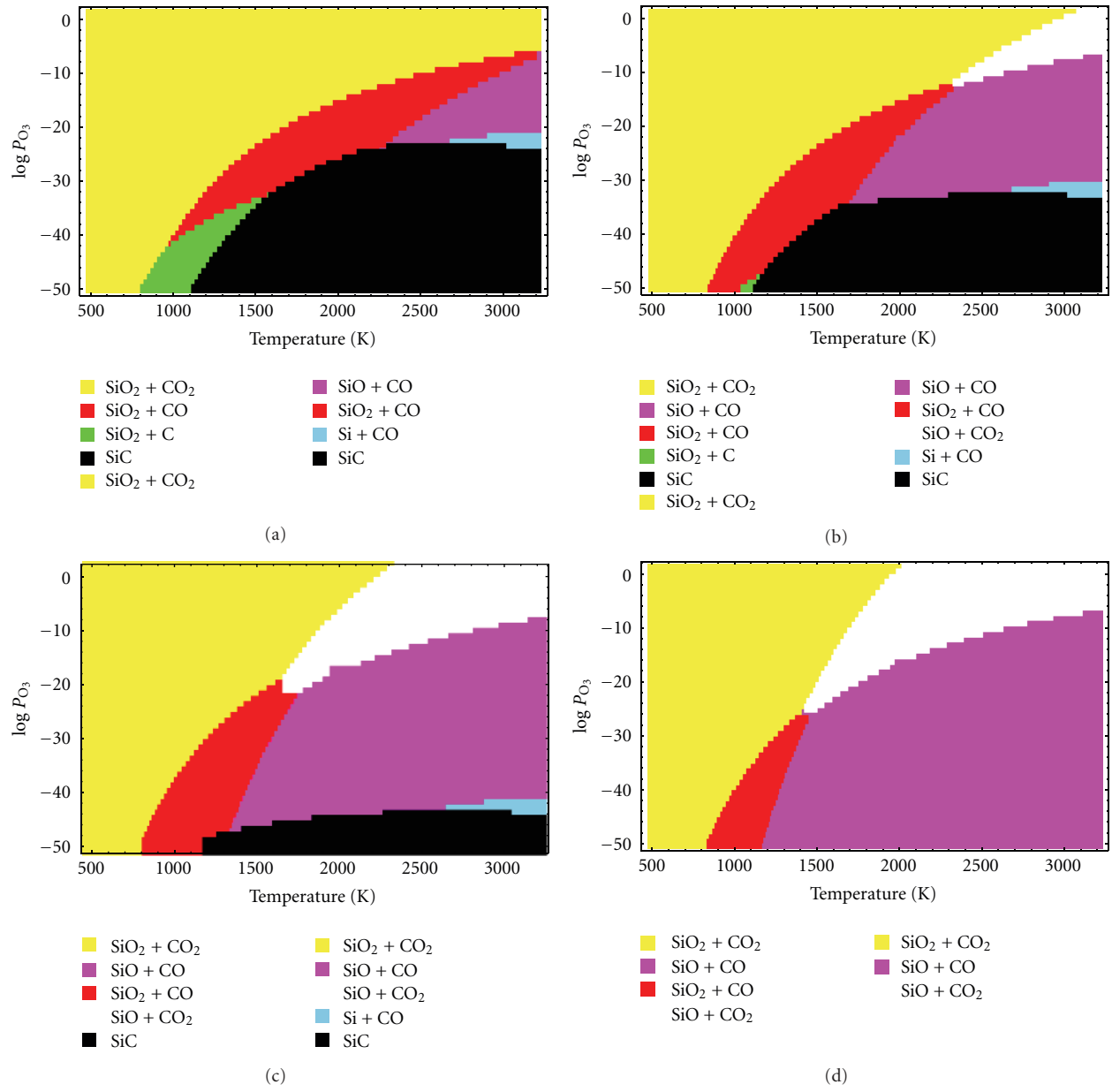

FIGURE 6: Equilibrium diagram of SiC oxidation with ozone (O_3) at (a) $\log P_{CO_2} = 0$, $\log P_{CO} = 0$, and $\log P_{SiO} = 0$, (b) $\log P_{CO_2} = -3$, $\log P_{CO} = -3$, and $\log P_{SiO} = -3$, (c) $\log P_{CO_2} = -7$, $\log P_{CO} = -7$, and $\log P_{SiO} = -7$, and (d) $\log P_{CO_2} = -10$, $\log P_{CO} = -10$, and $\log P_{SiO} = -10$.

atmosphere [17]. In other experimental observations on oxidations with molecular oxygen, SiO_2 has been observed to form a protective film on the surface of SiC between 900 and 1600°C [1]; this has been verified under reentry conditions [5]. Protective action reduces when SiO_2 begins to bubble at 3500 Pa and 1580°C [5]. Cracks form and become oxidation channels leading to rapid weight loss [13]. The oxidation behavior of the SiC indicated a two-step parabolic oxidation kinetics with formation of crystalline SiO_2 film. Diffusion of oxygen through the SiO_2 film becomes the rate-controlling step of reaction [18]. Charpentier et al. [19] observed with massive α-SiC samples that the transition between passive and active oxidation occurred at 1300 K for an oxygen partial pressure of 0.2 Pa and at 1600 K for 100 Pa. Our observation that the Si in SiC is more readily oxidized than the C is also corroborated by experimental studies [12] which show that even very small exposures to oxygen lead to an oxygenated Si terminated surface but without any change in the C-terminated surface.

4. Conclusions

Thermodynamics of oxidation reactions of SiC were studied by constructing a reaction equilibrium diagram of SiC

with atomic oxygen and ozone. Equilibrium constant (k)-temperature relations were derived for all the eight possible ways in which oxidation could occur. In all reactions, k values were observed to be highly positive and to decrease with temperature. The reaction forming $SiO_2 + CO_2$ was thermodynamically the most favourable. Partial pressure-temperature relations suggest that equilibrium pressures are extremely low.

Derived oxidation equilibrium diagrams showed the thermodynamically most favoured oxidation products and the sequence of oxidation under various conditions. As SiC was exposed to increasing levels of O or O_3, the first products were $SiO_2 + C$, followed by $SiO_2 + CO/SiO + CO_2$. High temperature and lower pressures of volatiles (CO, CO_2, and SiO) in the zone of oxidation favoured the formation of SiO over SiO_2. Moreover, in the SiC crystal, it is the Si atom which is more susceptible to oxidation than the C atom, and it is the Si which is first oxidized forming SiO_2.

Oxidation equilibrium diagrams could help to understand reactions during reentry of space vehicles. Since surface heating becomes significant at about 120 km from the Earth's surface, three layers of the atmosphere are involved, namely, the troposphere, stratosphere, and mesosphere-lower thermosphere. The SiO_2 layer (probably formed in the initial phase of re-entry) protects the bulk SiC from further catastrophic oxidation to SiO which could occur at higher temperatures at the later stages. Protective action towards oxidation would be effective till below the melting point of SiO_2 (1996 K), where upon SiO_2 liquid would be blown off the surface.

Acknowledgments

Financial support from ER & IPR, DRDO, and Government of India is gratefully acknowledged.

References

[1] P. J. Jorgensen, M. E. Wadsworth, and I. B. Cutler, "Oxidation of silicon carbide," *Journal of American Ceramic Society*, vol. 42, no. 12, pp. 613–616, 1959.

[2] M. Auweter-Kurtz, G. Hilfer, H. Habiger, K. Yamawaki, T. Yoshinaka, and H. D. Speckmann, "Investigation of oxidation protected C/C heat shield material in different plasma wind tunnels," *Acta Astronautica*, vol. 45, no. 2, pp. 93–108, 1999.

[3] Y. Song and F. W. Smith, "Effects of low-pressure oxidation on the surface composition of single crystal silicon carbide," *Journal of the American Ceramic Society*, vol. 88, no. 7, pp. 1864–1869, 2005.

[4] C. Virojanadara and L. I. Johansson, "Metastable oxygen adsorption on SiC(0001)-$\sqrt{3} \times \sqrt{3}$ R30°," *Surface Science*, vol. 519, no. 1-2, pp. 73–78, 2002.

[5] J. A. Costello and R. E. Tressler, "Oxidation kinetics of hot-pressed and sintered α-SiC," *Journal of the American Ceramic Society*, vol. 64, no. 6, pp. 327–331, 1981.

[6] P. Mogilevsky and A. Zangvil, "Modeling of oxidation behavior of SiC-reinforced ceramic matrix composites," *Materials Science and Engineering A*, vol. 262, no. 1-2, pp. 16–24, 1999.

[7] D. M. Liu, "Oxidation of polycrystalline α-silicon carbide ceramic," *Ceramics International*, vol. 23, no. 5, pp. 425–436, 1997.

[8] J. M. Powers and G. A. Somorjai, "The surface oxidation of alpha-silicon carbide by O_2 from 300 to 1373 K," *Surface Science*, vol. 244, no. 1-2, pp. 39–50, 1991.

[9] J. Wang, L. Zhang, Q. Zeng, G. L. Vignoles, and A. Guette, "Theoretical investigation for the active-to-passive transition in the oxidation of silicon carbide," *Journal of the American Ceramic Society*, vol. 91, no. 5, pp. 1665–1673, 2008.

[10] A. E. Mc Hale, Ed., *Phase Equilibria Diagrams, Phase Diagrams for Ceramists*, vol. 10, American Ceramic Society, Westerville, Ohio, USA, 1994.

[11] J. Weiss, H. L. Lukas, J. Lorenz, G. Petzow, and H. Krieg, "Calculation of heterogeneous phase equilibria in oxide-nitride systems. I. The Quaternary System C Si N O," *Calphad*, vol. 5, no. 2, pp. 125–140, 1981.

[12] J. W. Chamberlain and D. M. Hunten, *Theory of Planetary Atmospheres*, Academic Press, San Diego, Calif, USA, 1987.

[13] R. D. Thompson, *Atmospheric Processes and Systems*, Routledge, London, UK, 1998.

[14] M. W. Chase Jr., *NIST-JANAF Thermochemical Tables*, vol. 14 of *Journal of Physical and Chemical Reference Data*, AIP, New York, NY, USA, 1985.

[15] C. Varadachari, "Constructing phase diagrams for silicate minerals in equilibrium with an aqueous phase: a theoretical approach," *Soil Science*, vol. 153, no. 1, pp. 5–12, 1992.

[16] C. Varadachari, "Fuzzy phase diagrams of clay minerals," *Clays and Clay Minerals*, vol. 54, no. 5, pp. 616–625, 2006.

[17] T. Narushima, M. Kato, S. Murase, C. Ouchi, and Y. Iguchi, "Oxidation of silicon and silicon carbide in ozone-containing atmospheres at 973 K," *Journal of the American Ceramic Society*, vol. 85, no. 8, pp. 2049–2055, 2002.

[18] T. Narushima, T. Goto, and T. Hirai, "High-temperature passive oxidation of chemically vapor deposited silicon carbide," *Journal of the American Ceramic Society*, vol. 72, no. 8, pp. 1386–1390, 1989.

[19] L. Charpentier, M. Balat-Pichelin, and F. Audubert, "High temperature oxidation of SiC under helium with low-pressure oxygen-Part 1: sintered α-SiC," *Journal of the European Ceramic Society*, vol. 30, no. 12, pp. 2653–2660, 2010.